Science Signaling
AAAS

www.sciencesignaling.org/cgi/content/full/5/218/ra28/DC1

Supplementary Materials for

A Large Bioactive BMP Ligand with Distinct Signaling Properties Is Produced by Alternative Proconvertase Processing

Takuya Akiyama, Guillermo Marqués, Kristi A. Wharton*

*To whom correspondence should be addressed. E-mail: kristi_wharton@brown.edu

Published 3 April 2012, *Sci. Signal.* **5**, ra28 (2012)
DOI: 10.1126/scisignal.2002549

The PDF file includes:

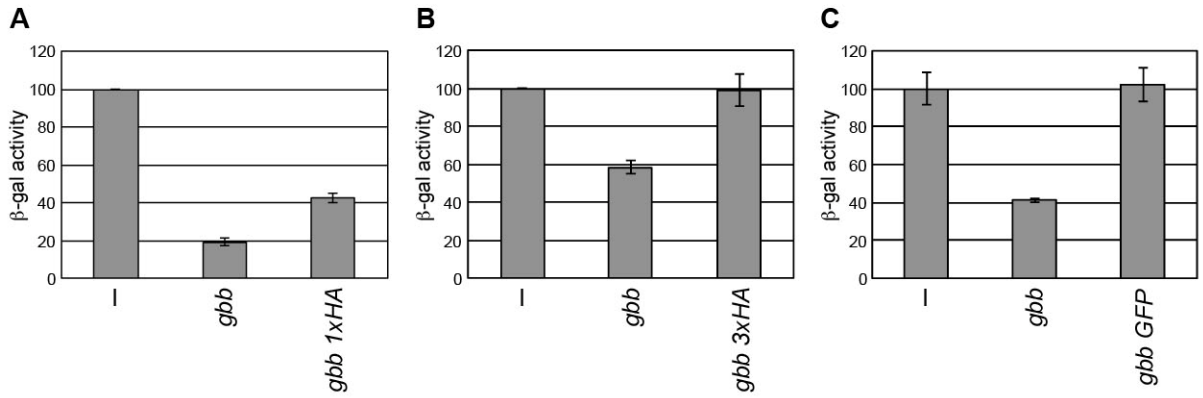

Figure S1. Signaling activity of the HA-tagged Gbb constructs.

(**A** to **C**) The biological activity of Gbb, Gbb-1xHA (A), Gbb-3xHA (B) and Gbb-GFP (C) were compared using the cell-based BMP signaling assay. Gbb-1xHA showed a slightly reduced signaling activity compared to Gbb, whereas Gbb-3xHA and Gbb-GFP had no BMP signaling activity.

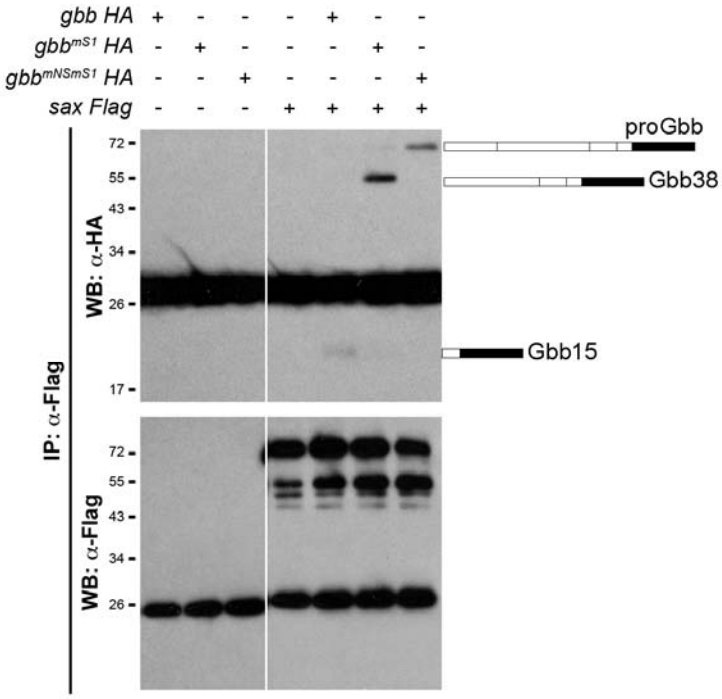

Figure S2. Gbb38 and Gbb15 bind to the Sax type I receptor.

Western blots of Gbb products that coimmunoprecipitate with Sax-Flag (top panel) and the receptor input fraction (bottom panel). Gbb products in coimmunoprecipitates were identified by anti-HA. Sax-Flag input identified by anti-Flag.

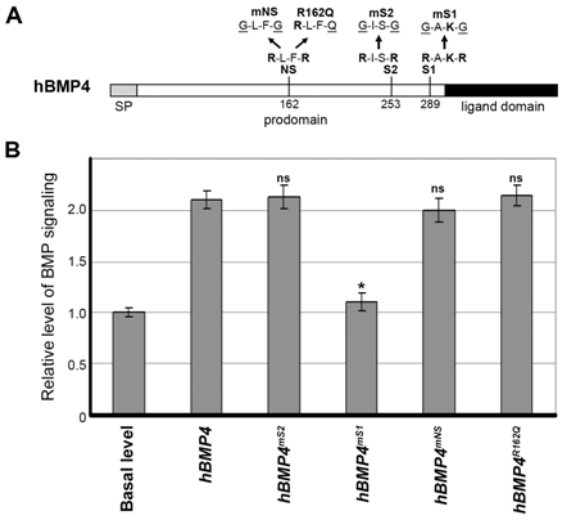

Figure S3. Signaling activity of the *hBMP4* and *hBMP4* cleavage mutants.
(**A**) Schematic illustration of hBMP4 pre-proprotein denoting the position of each furin cleavage sequence: NS, S2, and S1. Mutations to disrupt each cleavage site are shown above. $hBMP4^{R162Q}$ is associated with CLP. (**B**) The signaling activity of each CM and $hBMP4^{R162Q}$ were measured in HEK293 cells with the BRE-luciferase assay. Basal BMP signaling was set at 1. Four independent experiments were performed for each with error bars indicating SD. *, *P*-value<0.01. ns, not significantly different from hBMP4.

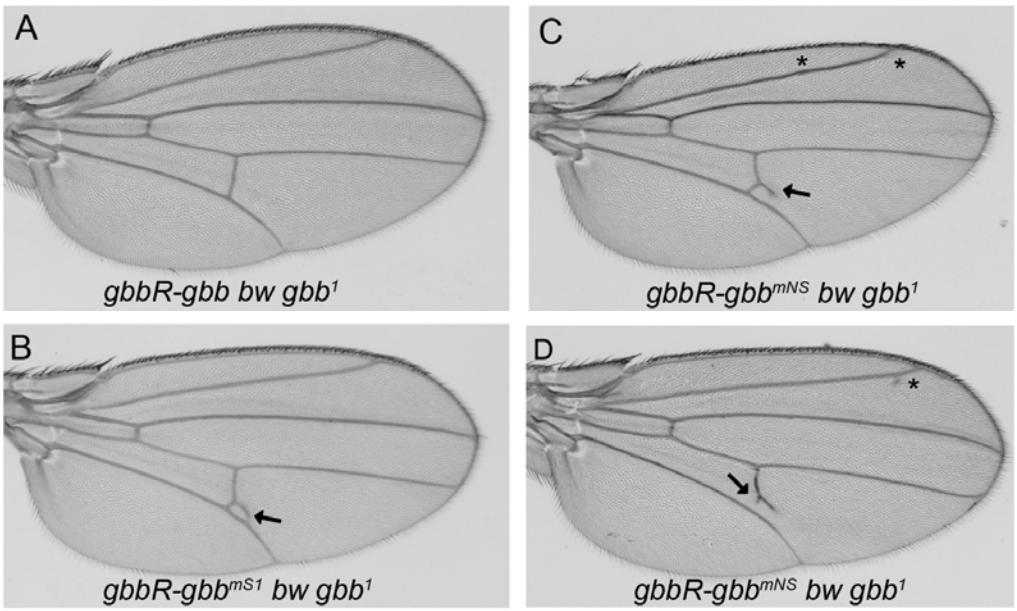

Genotype	WT	PCV spur	N	% wing defects
gbbR-gbb gbb^{1}	42	0	42	0
gbbR-gbb^{mNS} gbb^{1}	14	21	35	60
gbbR-gbb^{mS2} gbb^{1}	29	0	29	0

Figure S4. Failure to cleave Gbb at the NS results in wing defects.

Transgenic lines were generated with the insertion of a wild type *gbb* genomic rescue construct (*gbbR-gbb*) or a *gbb* rescue construct expressing one single cleavage mutants (*gbbR-gbb^{mS1}*, *gbbR-gbb^{mS2}*, and *gbbR-gbb^{mNS}*) in the same chromosomal position at 53B using the ϕC31 system. Lines for each construct were isolated and recombined onto a *gbb^{1}* null chromosome. (**A**) *gbbR-gbb bw gbb^{1}* homozygotes show complete rescue with a wild type wing pattern (N=447). (**B** to **D**) Wing defects consisting of ectopic vein material near the posterior cross vein (PCV, PCV spurs) were noted in homozygous survivors of both *gbbR-gbb^{mS1} bw gbb^{1}* (N=54) and *gbbR-gbb^{mNS} bw gbb^{1}* (N=35) (arrow; B, C, and D). *gbbR-gbb^{mNS} bw gbb^{1}* homozygotes exhibit a wavy longitudinal vein 2 with ectopic vein material along the vein (asterisks; C and D).

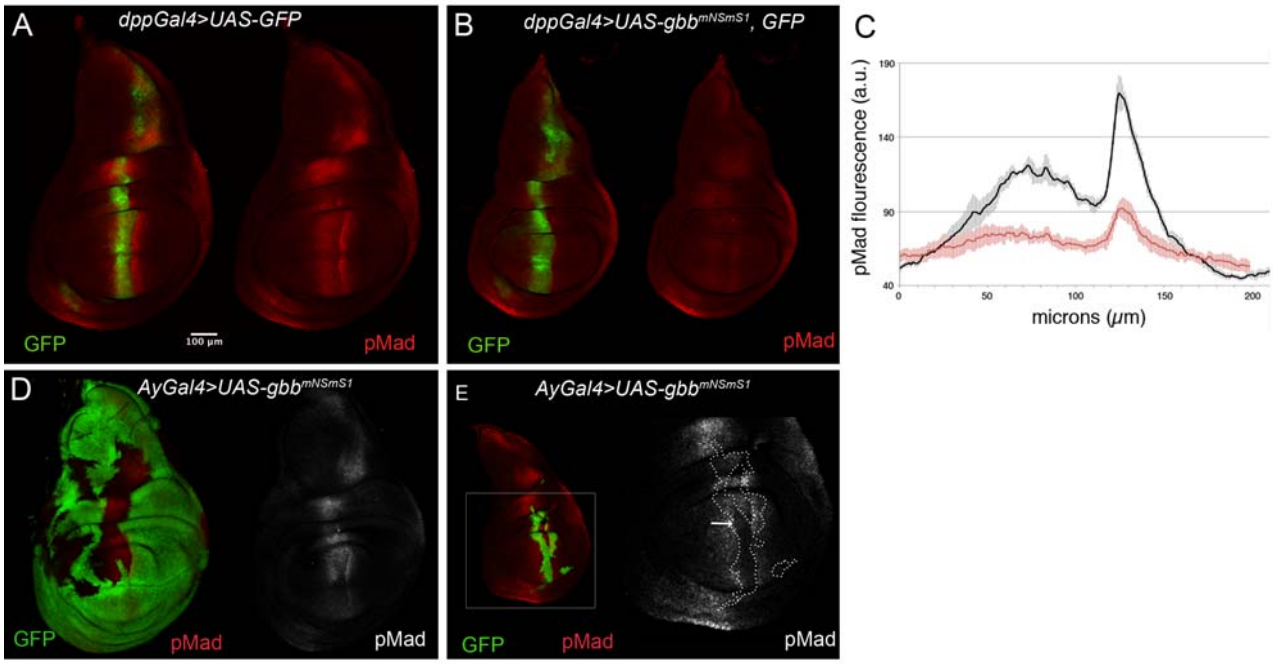

Figure S5. The *gbb* double cleavage mutant exhibits dominant-negative behavior when expressed in *dpp*-expressing cells of the wing imaginal disc.

The distribution of pMad (red; white (right panels in D and E) was examined in wing discs expressing the *gbb* double cleavage mutant (*UAS-gbbmNSmS1). UAS-GFP* was included in all crosses to mark the domain of expression. (**A**) *dppGal4>UAS-GFP*. (**B**) *dppGal4>UAS-gbb*^{mNSmS1} *UAS-GFP*. (**C**) Profiles of pMad fluorescence were plotted as an average of 4 wing discs from each genotype with standard errors (vertical lines). Each image used to obtain a pMad tracing is the sum of six 1µm confocal slices at equivalent positions along the Z axis. *dppGal4>UAS-GFP* (black); *dppGal4>UAS-gbb*^{mNSmS1} *UAS-GFP* (red). (**D** and **E**) FLP-OUT clones of *UAS-gbb*^{mNSmS1} were induced under the control of *actin-Gal4*. Right panels show pMad distribution in white. Magnification of the right panel in (E) is increased by 80%. Clone outline marked by dotted white line. Arrow denotes cells of clone with decreased pMad. Discs were imaged at same magnification. A&B and D&E were imaged at same confocal settings.

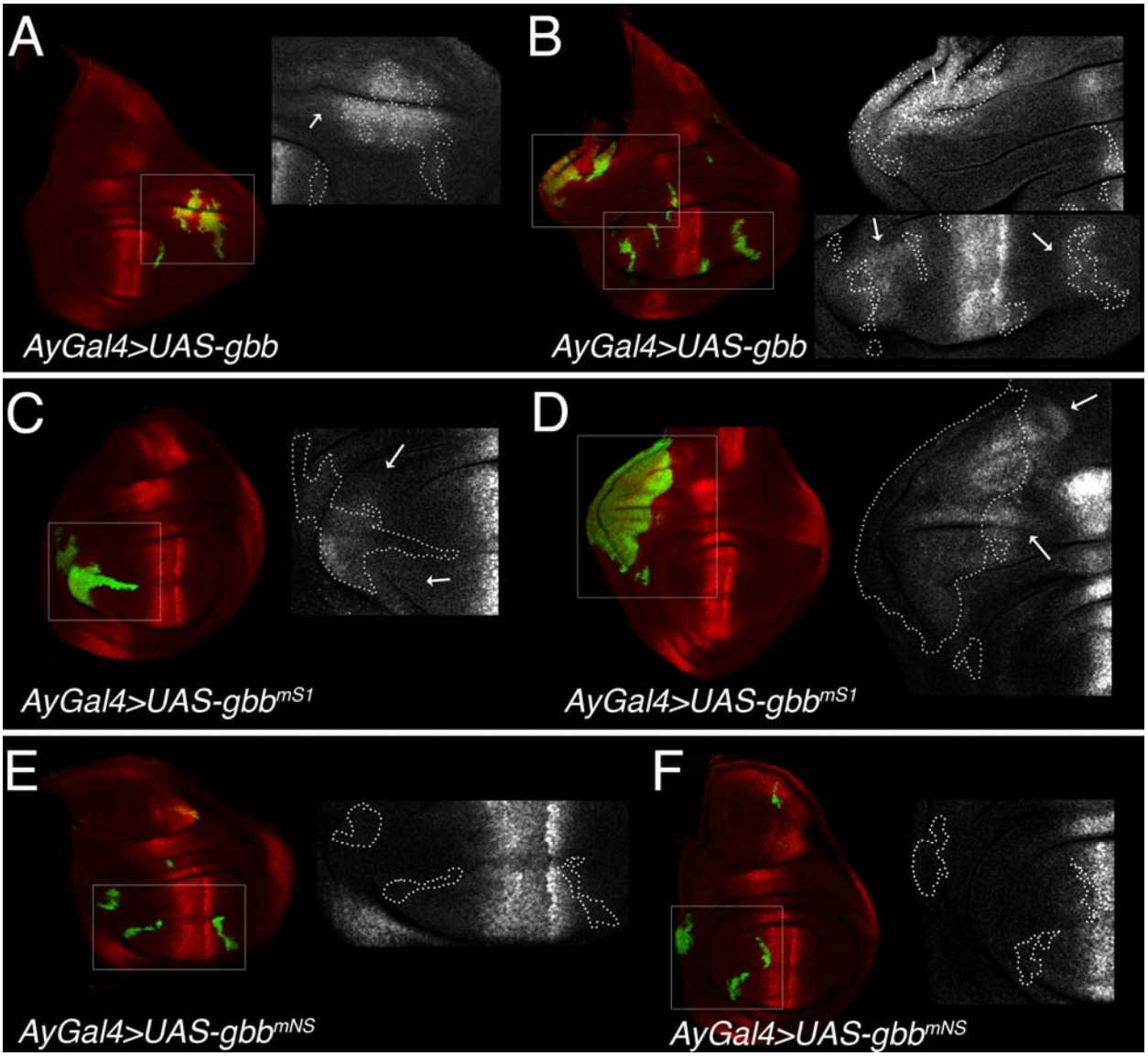

Figure S6. Wild-type *gbb* (Gbb38 and Gbb15) and *gbb*^{mS1} (Gbb38) exhibit nonautonomous signaling.

(**A** to **F**) pMad distribution (red) associated with FLPout clones expressing *gbb* (Gbb15 and Gbb38), *gbb*^{mS1} (Gbb38) or *gbb*^{mNS} (Gbb15) (green) (left panels). Boxed regions increased in magnification 2-fold, highlight clones (outlined in dotted line) and pMad signal (white) (right panels). Arrows mark presence of ectopic pMad outside the clone. (A) and (B), *AyGal4>UAS-gbb*. (C) and (D), *AyGal4>UAS-gbb*^{mS1}. (E) and (F), *AyGal4>UAS-gbb*^{mNS}.

Adults					
	N	Extra SA	Extra DC	Extra SC	
dpp>GFP	131.0	0 (0%)	0 (0%)	0 (0%)	
dpp>gbb	42.0	36 (49.3%)	22 (30.1%)	0 (0%)	
dpp>mNS	99.0	0 (0%)	0 (0%)	2 (1.3%)	
dpp>mS2	0.0	0 (0%)	0 (0%)	0 (0%)	
dpp>mS1	113.0	4 (2.3%)	0 (0%)	14 (8.1%)	
dpp>mNSmS1	0.0	0 (0%)	0 (0%)	0 (0%)	
Pharates					
	N	Extra SA	Extra DC	Extra SC	Leg defects
dpp>gbb	40.0	36 (90%)	26 (65%)	1 (2.5%)	17 (42.5%)
dpp>mNSmS1	25.0	0 (0%)	0 (0%)	20 (80%)	20 (80%)

Table S1. Macrochaetae and leg defects associated with misexpression of *gbb* and *gbb* cleavage mutants in *dpp*-expressing cells.

dppGal4>UAS-gbb and *dppGal4>UAS-gbbCM* adults were scored for the presence of notal macrochaetae defects. SA=supralar, DC=dorsocentral, and SC=scutellar macrochaetae. *dppGal4>UAS-gbb* and *dppGal4>UAS-gbb*^{mNSmS1} pharates were removed from their pupal cases and scored for abnormal macrochaetae. A high percentage of pharates were also found to exhibit short, bent, and/or misshapen pro-, meso- and metathoracic legs.

Genes	Primer sequences
gbb sense with *attB1*	5′-GGGGACAAGTTTGTACAAAAAAGCAGGCTAGATACACACAACAATCCGTAAGTGCG-3′
gbb anti-sense with *attB2*	5'-GGGGACCACTTTGTACAAGAAAGCTGGGTTCAATGGCACCCGCAGGATTTCACAA-3'
gbb[mNS] sense	5'-GGCCAT**G**GGTCCAGG**G**GGAGCGCC-3′
gbb[mNS] anti-sense	5'-GGCGCTCC**C**CCTGGACC**C**ATGGCC-3'
gbb[mS2] sense	5'-GTCAAC**G**GACCCGAC**G**GCGAGGTG-3'
gbb[mS2] anti-sense	5'-CACCTCGC**C**GTCGGGTC**C**GTTGAC-3'
gbb[mS1] sense	5'-CACCAC**G**GGAGCAAG**G**GAAGCGCC-3'
gbb[mS1] anti-sense	5'-GGCGCTTC**C**CTTGCTCC**C**GTGGTG-3'
gbb sense with *EcoR*I	5'-GGCGGCgaattcAAGATACACACAACAATCCGTAAGTGC-3'
gbb anti-sense with *Xba*I	5'-GGCGGCtctagaTCAATGGCACCCGCAGGATTTC-3'
hBMP4 sense	5′-GGGGACAAGTTTGTACAAAAAAGCAGGCTaagcttAAGCTTGCCGCCACCATGATTCCTGGTAACCG AATGCTGATG-3'
hBMP4 anti-sense	5'-GGGGACCACTTTGTACAAGAAAGCTGGGTctcgagTCAGCGGCACCCACATCCCTCTACTAC-3'
hBMP4[mNS] sense	5'-CGAGGTGATCTCCTCTGCAGAGCTT**G**GGCTCTTC**G**GGGAGCAGGTGGACCAGGGCCCTG-3'
hBMP4[mNS] anti-sense	5'-CAGGGCCCTGGTCCACCTGCTCCC**C**GAAGAGCC**C**AAGCTCTGCAGAGGAGATCACCTCG-3'
hBMP4[R162Q] sense	5'-CGAGGTGATCTCCTCTGCAGAGCTTCGGCTCTTCC**A**GGAGCAGGTGGACCAGGGCCCTG-3'
hBMP4[R162Q] anti-sense	5'-CAGGGCCCTGGTCCACCTGCTCC**T**GGAAGAGCCGAAGCTCTGCAGAGGAGATCACCTCG-3'
hBMP4[mS2] sense	5'-GGCCAGCATGTC**G**GGATTAGC**G**GATCGTTACCTC-3'
hBMP4[mS2] anti-sense	5'-GAGGTAACGATC**C**GCTAATCC**C**GACATGCTGGCC-3'
hBMP4[mS1] sense	5'-GCCTTGACCCGACGCCGG**G**GGGCCAAG**G**GTAGCCCTAAGC-3'
hBMP4[mS1] anti-sense	5'-GCTTAGGGCTAC**C**CTTGGCCC**C**CGGCGTCGGGTCAAGGC-3'

Table S2. Primers used in this study.

attB1 and *attB2* DNA sequences are underlined. Bold characters indicate point mutations and lowercase characters highlight restriction sites.